

Compatibility of Infrared Band Models with Scattering

R. A. Reed,* D. G. Brown,† R. S. Hiers III,† B. K. Cromwell,† and V. A. Zaccardi†
Sverdrup Technology, Arnold Air Force Base, Tennessee 37389

Techniques for the computation of radiative heating from aluminized solid propellant rocket exhaust plumes must account for infrared emission and absorption by hot H_2O and CO_2 in the presence of strong three-dimensional aerosol scattering by micron-sized Al_2O_3 droplets and particles. Radiative heating computations are usually performed over wide spectral intervals using infrared band models. However, no rigorous extension to infrared band models has been proposed for situations with scattering. Indeed, band models and scattering are widely held to be incompatible. Practical engineering calculations of plume radiative heating have therefore proceeded, using various approximations to the transport equation. Although the errors in these approximations are believed to be reasonably small, they have never been quantified because of the lack of rigorous results. In order to help remedy this deficiency, this article develops two different rigorous solutions. Although they are currently restricted to homogeneous media, they nevertheless provide a previously unavailable means of calibrating code performance and assessing the accuracy of various approximation schemes. Some sample applications are provided for the Space Shuttle Solid Rocket Booster.

Introduction

THE objective of this article is to show that rigorous infrared band model solutions to the full radiative transport equation including scattering can be found, at least for homogeneous media. These solutions can be helpful if one needs to assess the accuracy of various plume radiation codes or to choose between several alternative methods. Techniques for the computation of rocket exhaust plume radiative heating were first developed for the large RP1-LOX launch vehicles used in the early 1960s. For combined reasons of computational efficiency and lack of adequate high-temperature line-by-line spectral compilations, these techniques rely upon infrared band models. A typical plume calculation can require the evaluation radiance inside a double loop composed of 1000 wavelengths at each of 100–200 lines of sight. Computational efficiency is therefore important. Band models provide spectral data for the polyatomic combustion gases such as water vapor and carbon dioxide at spectral resolutions of typically $5\text{--}10\text{ cm}^{-1}$, although much coarser resolution is often acceptable for radiative heat transfer. The conventional infrared band model treatment^{1–3} does not consider scattering, and is based upon a one-dimensional line-of-sight integration of the radiative source function. Assuming local thermodynamic equilibrium, the source function is simply the Planck radiation function. When scattering occurs, however, the radiative transport becomes three-dimensional. This is because the source function now contains contributions due to radiance emitted from adjacent volume elements and scattered into the line of sight. In addition, when one attempts to perform a band model frequency average of the transport equation, scattering adds higher-order terms to the source function involving frequency correlations. The result is that the conventional infrared band model formalism fails under these conditions. For hydrogen-oxygen and amine fueled rockets, the exhaust is purely gaseous and the band model formalism applies directly. On the other hand, for RP1-LOX and aluminized solid propellants, the exhaust contains condensed

phases which complicate the radiance calculation. In the case of RP1-LOX, the condensed phase is carbon soot. For soot particles much smaller than the wavelength, scattering can be neglected and the absorption can be readily incorporated into a band model. For aluminized fuels, both liquid droplets and solid particles of aluminum oxide in the exhaust are efficient scatterers of radiation from visible wavelengths to about $5\text{ }\mu$ in the midinfrared. The intense thermal plume emission as exemplified in Fig. 1, measured from a $\frac{1}{8}$ -scale 110,000-lbf thrust Space Shuttle Solid Rocket Booster (SRB) fired at NASA Marshall Space Flight Center, is therefore strongly influenced by multiple scattering. The absorption band near 2350 cm^{-1} is due to carbon dioxide. The others near 7200 , 5200 , and 3700 cm^{-1} are primarily due to water vapor.

Typical radiative transport properties in an aluminized solid propellant exhaust plume are illustrated in Fig. 2. These particular curves are for the Space Shuttle SRB exhaust plume at sea level. The propellant for this motor is 16% aluminum by weight. However, the results would be similar for any highly aluminized propellant, regardless of motor size. The figure shows the separate contributions to the plume opacity from water vapor, CO_2 , and Al_2O_3 scattering and absorption. The gas opacities are 5 cm^{-1} band model parameters based upon an upgrade⁴ of the NASA compilation.¹ If the line-by-line absorption coefficients were shown, the gas opacity at the center of the strongest lines would probably exceed the particle opacity. Similarly, the trough regions between lines would also be deeper. Additional opacity contributions due

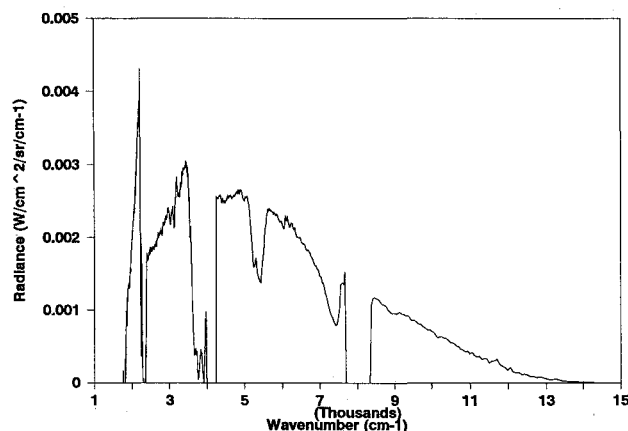


Fig. 1 Measured exit plane spectrum of $\frac{1}{8}$ -scale Space Shuttle SRB.

Presented as Paper 92-2891 at the AIAA 27th Thermophysics Conference, Nashville, TN, July 6–8, 1992; received July 13, 1992; revision received Sept. 24, 1993; accepted for publication Oct. 6, 1993. This paper is declared a work of the U.S. Government and is not subject to copyright protection in the United States.

*Engineering Specialist, AEDC Group.

†Engineering, AEDC Group.

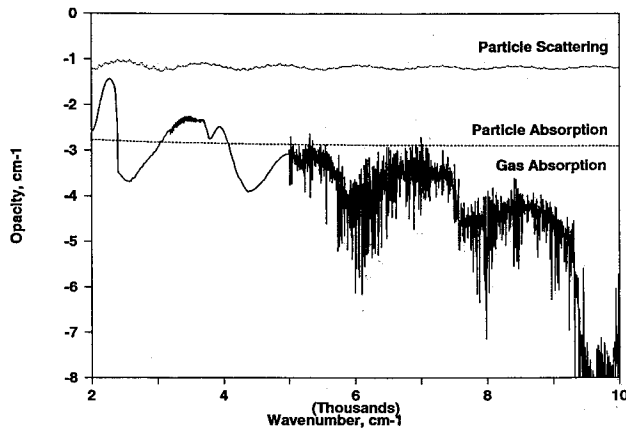


Fig. 2 SRB opacity contributions.

to CO and HCl also occur, but are not shown. A nominal temperature of 2400 K was used and an Al_2O_3 droplet radius of 5.8 μm was employed, based upon the Hermesen size correlation.⁵ The Al_2O_3 droplet scattering and absorption were calculated using the BHMIE code.⁶ The real part of the refractive index was based upon the 633-nm data of Krishnan et al.⁷ and scaled with wavelength according to the measurements of Gryvnak and Burch.⁸ The imaginary part of the refractive index was based upon the data of Refs. 9 and 10. Since some of the SRB alumina is predicted to be in the less emissive solid form,¹¹ the Al_2O_3 absorption shown in the figure is probably an upper bound. The multiphonon absorption^{12,13} below 2500 cm^{-1} was not included, so the particle absorption curve is an underestimate in this spectral region. The main point of Fig. 2 is that scattering is the dominant transport process. Even in the strong 2300 cm^{-1} CO_2 and 3700 cm^{-1} H_2O bands, the band-averaged gas absorption does not exceed droplet scattering. The need to accurately incorporate the effects of scattering is evident. However, this greatly complicates the formulation of the infrared band model.

Band Model—Scattering Incompatibility

Although Malkmus¹⁴ and Domoto¹⁵ mention the incompatibility of scattering and band models, neither gives an explicit account. This section therefore presents a highly simplified summary of conventional infrared band models and why they fail in the presence of scattering. Only homogeneous paths are considered here. The formal solution to the monochromatic (i.e., single frequency) radiative transport equation in terms of dimensionless optical depth τ_ν is

$$I_\nu(\tau_\nu, \Omega) = \int_\tau^\infty e^{-(\tau_\nu - \tau'_\nu)} S(\tau'_\nu, \Omega) d\tau'_\nu \quad (1)$$

where $I_\nu(\tau_\nu, \Omega)$ is the radiance and $S(\tau_\nu, \Omega)$ is the source function. The subscript ν on these three terms indicates the frequency dependence, and Ω is the angular coordinate. The optical depth includes one contribution k_ν from the gas with fine spectral structure (line widths are on the order of 0.1 cm^{-1}), and another $n\sigma_e$ from the particles or droplets which varies only slowly with frequency. The frequency subscript on the latter is therefore omitted. In terms of path length s , the optical depth τ is

$$\tau_\nu = (k_\nu + n\sigma_e)s \quad (2)$$

where n is the particle concentration and σ_e is the particle extinction cross section, defined as the sum of the absorption and scattering cross sections:

$$\sigma_e = \sigma_a + \sigma_s \quad (3)$$

With these definitions, the source function (for equal gas and particle temperatures) is

$$S_\nu(\Omega) = (1 - \omega_\nu)B + \omega_\nu \int P(\Omega - \Omega') I_\nu(\Omega') d\Omega' \quad (4)$$

where the spatial dependence of the variables has been suppressed for simplicity. B is the Planck function, which like σ_e is essentially constant over small spectral intervals, and ω is the volume scattering albedo

$$\omega_\nu = n\sigma_s / (n\sigma_e + k_\nu) \quad (5)$$

The kernel of the scattering integral is the scattering phase function $P(\Omega)$, and the angular integral is performed over 4π sr. In the absence of scattering, the ω is zero, and the source function equals the Planck function, $S = B$. In the absence of scattering, the emissivity ϵ_ν , which is simply the ratio of I_ν to the Planck function B , is simply

$$\epsilon_\nu = 1 - T_\nu \quad (6)$$

where the transmissivity T_ν is related to optical depth by

$$T_\nu = e^{-\tau_\nu} = e^{-k_\nu s} \quad (7)$$

For many engineering applications one needs a solution only for the emissivity $\bar{\epsilon}_\nu$ averaged over a fairly wide spectral band $\Delta\nu$, centered at frequency ν , and containing many spectral emission lines. In the absence of scattering this simply involves the spectral average of a single term, the transmissivity, since by Eq. (6)

$$\bar{\epsilon}_\nu = 1/\Delta\nu \int_{\nu - \Delta\nu/2}^{\nu + \Delta\nu/2} \epsilon_\nu d\nu = 1 - \bar{T}_\nu \quad (8)$$

The essential point of infrared band models is that the integral of Eq. (8) can be evaluated solely from the statistical properties of the spectral lines. It is not necessary to know the detailed frequency spectrum of either the emission ϵ_ν or the transmission T_ν . Defining a quantity $f_\nu(k)$ as the probability distribution of gas opacity k over the band $\Delta\nu$, centered at frequency ν , the fundamental band model result can be expressed as

$$\bar{T}_\nu = \int_0^\infty e^{-k} f_\nu(k) dk \quad (9)$$

Band model parameters and formulas have been tabulated for a large number of gases as a function of temperature, pressure, and mean frequency. Extensive validations against experimental data have also been performed, and the band model result Eq. (9) agrees well with the direct result Eq. (8) in cases where the detailed transmission spectrum is known. The band model method has also been extended to inhomogeneous paths.

When scattering is added to the radiative transport equation, inspection of Eqs. (1) and (4) shows that, in addition to becoming three-dimensional, the transport equation also involves higher-order correlation terms proportional to

$$\overline{\omega_\nu T_\nu} \quad \text{and} \quad \overline{\omega_\nu I_\nu T_\nu} \quad (10)$$

The approach in practical band model calculations with scattering has been to approximate these terms in the transport equation by uncorrelated products of the form

$$\overline{\omega_\nu} \bar{T}_\nu \quad \text{and} \quad \overline{\omega_\nu} \bar{I}_\nu \bar{T}_\nu \quad (11)$$

Rigorous procedures for handling the correlations in terms like Eq. (10) have not been developed because these terms

depend upon the mixing ratio of gas to particles, and therefore, cannot be tabulated like conventional band model parameters for pure gases. In addition, the triple correlation involves the radiance I_r , which is not defined explicitly by the transport equation. Collectively, these difficulties constitute what is generally known as the band model—scattering incompatibility problem.

Review of Earlier Work

The earliest attempts to model radiation from aluminized solid propellant rocket exhaust plumes disregarded scattering altogether. Aluminum oxide absorption opacity was simply added to the gas opacity in the same way as for soot. At high optical depths, however, this fails because the gas and particle emissivities are not additive. A number of investigators therefore proposed band model solutions including scattering, all of which were based upon various approximations to the transport equation. Vanderbilt and Slack¹⁶ provided the first practical band model treatment for plumes using the classic two-flux technique.¹⁷ The treatment was strictly one dimensional. Malkmus¹⁴ attempted to place this solution on a more rigorous basis by providing a proper band model average for the terms referred to in Eq. (8). Among other things, he demonstrated an unusual cube root region to the curve of growth. It was not determined whether this would actually occur in a plume or whether it was a result of the one-dimensional assumption. Ludwig et al.¹⁸ provided a three-dimensional solution based upon the six-flux approximation.^{19,20} The solution was based upon a series expansion of radiance in terms of successive orders of scattering (i.e., the Neumann series solution). A band model spectral average was performed only for the leading term, i.e., unscattered emission. The other terms involving scattering were evaluated using Beer's law, which is inapplicable to band models. Everson and Nelson²¹ performed three-dimensional Monte Carlo radiative transport calculations using a band model curve of growth with 400 cm^{-1} spectral resolution, again without treating the higher-order correlation terms in Eq. (11). Although not decisive, the fair agreement between these various approximations indicates that they are probably adequate for engineering design. However, an accurate error assessment against exact test cases is nevertheless highly desirable. The major point of this article is to show that the classical band model approach for gases can be rigorously extended to simple scattering problems, so that rigorous test cases can be generated for certain simple benchmark test cases.

Monte Carlo Radiative Transport Calculations

Infrared band models are based upon a statistical average of the monochromatic solution to the radiative transport equation. In the absence of scattering, the monochromatic solution is a simple analytic function, as indicated in Eq. (7). In the presence of scattering, the monochromatic solution is generally much more complex. However, once obtained, it can be statistically averaged just as for the nonscattering case. A representative summary of solution techniques for the monochromatic scattering problem is given by Crosbie and Linzenhardt.²² The Monte Carlo technique was used in this study because of its ease in coding and versatility. However, the rigorous band model—scattering solution demonstrated in subsequent sections of this article is in no way tied to the Monte Carlo method. A numerical method would have worked just as well. Comparison of our Monte Carlo with results from the doubling method for the directional reflectivity and emissivity of anisotropic scattering slabs²³ shows agreement within the expected standard deviation. This is on the order of 1% for 10^4 photons. In the present investigation, the ability of the Monte Carlo code to track the photon path length distribution or to separately record the scattered and unscattered radiance was especially convenient.

The capabilities of the Monte Carlo code include general two-dimensional plume geometry with multiple radial zones

and a conical expansion along the thrust axis.²⁴ However, all of the calculations in this article were made for homogeneous cylindrical plumes. The scattering phase function was the Henyey-Greenstein function.^{25,26} This is an analytical approximation to the Mie scattering phase function. It lacks the fine-scale oscillatory structure and the backscatter lobe near 180 deg, but is otherwise a convenient representation of the full Mie result, especially for polydispersions. An additional advantage to using the Henyey-Greenstein function is the availability of extensive tables of numerical results²³ for code validation. The one free parameter of this scattering function specifies the degree of forward scattering. Specifically, it is the mean cosine of the scattering angle. In principle, the Monte Carlo code could equally well use the full Mie scattering phase function. However, the particle shape and size distribution in rockets is sufficiently uncertain⁵ that using the full Mie scattering phase function is unwarranted.

For calculating the radiance into a specified line of sight, the backward Monte Carlo method is fastest. Mathematically speaking, the backward method solves the adjoint radiative transport problem. The equivalence of the backward and the direct solutions is called the reciprocity theorem^{27,28} or theorem of optical mutuality.²⁹ Physically, the backward Monte Carlo can be justified using Kirchhoff's law and microscopic reversibility.

Rocket Exhaust Plume Model

Since the importance of multiple scattering increases with optical depth, a large exhaust plume is the most difficult case for code prediction. The Space Shuttle SRB was therefore selected for this initial investigation. The exhaust plume was approximated by a homogeneous cylinder 1.90 m in radius and 60 m in length. Temperature, pressure, water vapor, and Al_2O_3 mole fractions were taken from a one-dimensional kinetic nozzle code calculation.³⁰ The mean particle radius of $5.8 \text{ }\mu\text{m}$ was based upon the Hermesen particle size correlation.⁵ The scattering asymmetry factor g was computed using the BHMIE code⁶ for a range of wavelengths and particle sizes. It varied by about only 0.1 from the nominal value of 0.7, so the latter value was used throughout the calculation. For relevance to vehicle base heating, a forward-looking line of sight was selected with an aspect angle of 30 deg to the thrust axis. This line of sight intersected the plume boundary two-nozzle exit radii downstream of the nozzle exit plane and passed through the plume centerline. The particle absorption was set to zero to maximize scattering and thereby provide a more challenging test case. Photon paths leaving the plume at the forward nozzle end of the cylinder were not considered to contribute to the overall emissivity. Very few photons fell into this category. Figure 3 shows the total monochromatic emissivity of the simulated cylindrical SRB plume as a function of the gas absorption coefficient. This curve was calculated using the backward Monte Carlo technique. The relative

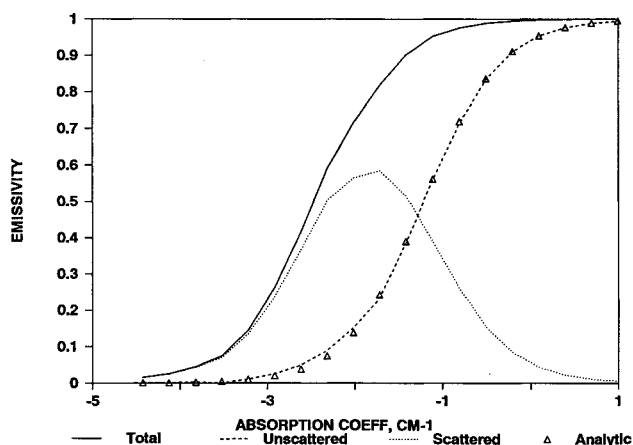


Fig. 3 Space Shuttle SRB emissivity.

proportions of unscattered vs scattered radiation are also shown on the plot. For values of the absorption coefficient less than approximately 0.1 cm^{-1} , most of the gas emission is scattered one or more times before leaving the plume. This will generally be the case for H_2O and CO_2 emission from the SRB plume. The unscattered radiance can be obtained analytically by the integration of Eq. (1), by using only the thermal emission component of the source function $(1 - \omega)B$, under the integral sign. As can be seen, the Monte Carlo estimate for unscattered emission (dashed line) agrees well with this analytic result (triangles). It should be emphasized that the curves in Fig. 3 are not universal. They must be calculated anew for each line of sight and each new plume. We now move to the main point of this article, which is to extend the monochromatic solution with scattering to a rigorous band result, i.e., without making any approximations to the radiative transport equation.

Solution Method No. 1

The first closed form solution was proposed by Domoto,¹⁵ but never actually implemented. The essence of his result is as follows. The band model transmissivity $T(s)$ averaged about some mean frequency ν is defined by the integral:

$$\overline{T_\nu(s)} = 1/\Delta\nu \int_{\nu_0 - \Delta\nu/2}^{\nu_0 + \Delta\nu/2} e^{-k_\nu s} d\nu \quad (12)$$

where s denotes path length, k_ν is the spectral absorption coefficient, and $\Delta\nu$ is a frequency interval on the order of $5\text{--}25 \text{ cm}^{-1}$ wide. The band model emissivity is equal to $1 - T(s)$. Domoto noted that since the functional dependence of emissivity is upon the absorption coefficient k , and not upon the frequency ν , one could obtain the same result as Eq. (9) using an absorption probability distribution function $f_\nu(k)$, the latter quantity defined within a band of spectral width $\Delta\nu$ and centered about ν :

$$\overline{T_\nu(s)} = \int_0^\infty e^{-ks} f_\nu(k) dk \quad (13)$$

The exponential factor in Eq. (10) is simply the Beer's law transmissivity, which always applies in the monochromatic case. Inspection of Eq. (10) shows that the desired probability distribution $f(k)$ is simply the inverse Laplace transform of the band model transmissivity function $T(s)$. Therefore, the traditional band model average of any quantity $g(k_\nu)$ in the frequency domain can be replaced by a corresponding average in the k domain weighted by $f_\nu(k)$. Specifically, Domoto showed that the band model spectral average of any function g_ν

$$\overline{g_\nu} = 1/\Delta\nu \int_{\nu_0 - \Delta\nu/2}^{\nu_0 + \Delta\nu/2} g(k_\nu) d\nu \quad (14)$$

could be evaluated in the k domain using the opacity distribution function $f_\nu(k)$:

$$\overline{g_\nu} = \int_0^\infty g(k_\nu) f_\nu(k) dk \quad (15)$$

If one chooses $g(k_\nu)$ to be the monochromatic radiance solution to the radiative transport equation in the presence of scattering, then Eq. (15) provides a simple procedure to extend this to a rigorous band model result. The function $f_\nu(k)$ is determined by the statistical properties of the spectral lines and the line broadening mechanism. For the widely used exponential-tailed $1/S$ band model of Malkmus³¹ and collision broadened lines, an analytic result for $f_\nu(k)$ is known¹⁵:

$$f_\nu(k) = \sqrt{(\kappa\alpha/\pi k^3)} e^{\alpha(2 - \kappa/k - k/\kappa)} \quad (16)$$

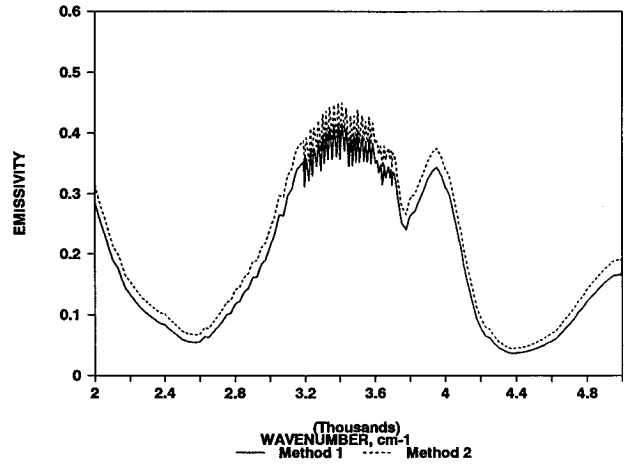


Fig. 4 Rigorous solution: method 1 vs method 2.

Frequency subscripts on the band model parameters and κ have been omitted for simplicity in Eq. (16). The first band model parameter is κ and is the optically thin limit of the absorption coefficient. It is also called S/d , where S is the mean line strength and d the mean line spacing. Alpha, α , is the second band model parameter and is the ratio of line half-width to mean line spacing d . Based upon the line broadening coefficients¹ and the SRB species mole fractions,³⁰ a collision half-width of 0.027 cm^{-1} was used. To generate a band model spectrum, H_2O band model tabulations¹ of d and κ were used to generate $f_\nu(k)$, according to Eq. (16) at 5-cm^{-1} intervals. This was converted to a band model result according to Eq. (15), using the monochromatic emissivity plotted in Fig. 3 as the function $g(k)$. The result is labeled as method no. 1 in Fig. 4. It is a rigorous band model result because the only errors are numerical and statistical. It makes no approximations whatsoever to the transport equation.

Solution Method No. 2

The second solution provides an alternative method that is convenient whenever the absorption coefficient $f_\nu(k)$ is not known or is difficult to determine. The form of the result is also more closely related to practical band model parameters. Consider, e.g., that the water vapor lines in the SRB plume have a Doppler width of approximately 0.015 cm^{-1} . Since this is more than half of the 0.027-cm^{-1} collision width, the water lines really have a Voigt profile. The analytical result of Domoto for collision broadened lines [Eq. (13)] no longer applies, and a more general solution is needed.

Let $g(k)$ be the monochromatic quantity to be averaged, and $h(s)$ its inverse Laplace transform:

$$g(k) = \int_0^\infty h(s) e^{-ks} ds \quad (17)$$

Substitution of Eq. (14) for $g(k)$ into Eq. (12) gives a double integral over path length s and absorption coefficient k . Reversing the order of integration and performing the k integral transforms $f(k)$ back into $T(s)$, according to Eq. (10). This gives the second solution. It is essentially the Laplace transform equivalent of Eq. (15):

$$\overline{g} = \int_0^\infty h(s) T(s) ds \quad (18)$$

According to Eqs. (12) and (15), one has the option of performing the band model average of any given function $g_\nu(k)$ in two equivalent ways. The first is to perform the average in k space, using the opacity $f_\nu(k)$ as in Eq. (15). The second is to perform the average in the Laplace transform domain, using $T(s)$ as in Eq. (18). A principal advantage of the second

solution is that infrared band model formulas for the transmissivity vs path length $T(s)$ are readily available, whereas formulas for the opacity distribution (solution 1) generally are not. The second solution is also advantageous when the total transmissivity is expressed as a product of two or more transmission factors. This occurs, e.g., for overlapping water and CO_2 bands, and for the multiple line group formalism.^{1,18}

The inverse transform $h(s)$ for transmission has a simple physical interpretation in at least two cases. The first is the trivial case in which no scattering occurs. In this case $g(k_\nu)$ is given by Beer's law

$$g(k_\nu) = e^{-k_\nu s_0} \quad (19)$$

where s_0 is the path length along the line of sight. The inverse Laplace transform of this is a delta function at s_0 :

$$h(s) = \delta(s - s_0) \quad (20)$$

Substitution of this $h(s)$ into Eq. (15) returns the pure gas band model transmissivity at s_0 , $T(s_0)$, as expected.

The second case where $h(s)$ has a direct physical interpretation is for a homogeneous absorbing gas with scattering. The scatterers themselves do not need to be homogeneous. In this case $h(s)$ is the photon path length probability distribution function $P(s)$. Specifically, the monochromatic emissivity $\epsilon(k_\nu)$, and the path length distribution function $P(s)$, obey a Laplace transform relationship:

$$\epsilon(k_\nu) = 1 - \int_0^\infty P(s) e^{-k_\nu s} ds \quad (21)$$

As discussed by van de Hulst,²³ $P(s)$ is the normalized probability distribution of photon path lengths in the absence of absorption. The path length variable s includes all the zigs and zags of the photon scattering trajectory. It can, and often does, exceed the physical size of the medium. Equation (21) can be intuitively recognized as a generalization of Eqs. (6) and (7) to the case when many different ray paths contribute to the emission. In the absence of scattering, $P(s)$ collapses to a delta function at s_0 . One therefore regains Beer's law in the monochromatic case, and the conventional band model transmissivity $T(s_0)$ in the spectrally averaged case.

The path length distribution function $P(s)$ for the SRB was evaluated by setting all absorption in the plume to zero and recording the path length of 300,000 Monte Carlo photons in histogram form. The result is shown in Fig. 5. The path length along the direct line of sight path is 760 cm. The mean path length with scattering is 337 cm, but many paths exceed 1000 cm. The smooth line is a cubic curve fit to the histogram. As a consistency check on the curve fit, it was verified that $P(s)$ and the monochromatic emissivity $\epsilon(k)$ obeyed the Laplace transform relationship Eq. (18). To demonstrate the equiv-

alence of the new solution with Domoto's result, Eq. (15), the integral indicated in Eq. (15) was carried out using $h(s) = P(s)$. For internal consistency, the transmissivity $T(s)$ for the same exponential-tailed $1/S$ random band model was used³¹:

$$T(u) = -2\alpha[\sqrt{1 + \kappa u/d} - 1] \quad (22)$$

The path length variable u is a column density which accounts for the water vapor partial pressure (H_2O), temperature T , and physical path length s :

$$u = s(\text{H}_2\text{O}) (273 \text{ K}/T) \quad (23)$$

As can be seen from the curve marked method no. 2 in Fig. 4, the solution obtained in this way is the same, at least to within numerical accuracy, as for the previous solution. The slight difference is attributed to an overestimate of the amplitude of $P(s)$ for large values of s , where the Monte Carlo statistics are sparse.

Whereas, the examples of Fig. 4 are for purely scattering particles, real alumina exhaust particles absorb as well as scatter. This is easily treated because particle absorption is mathematically indistinguishable from a gray gas absorption with coefficient $k_p = n\pi r^2 Q_a$. Here, n is the particle number density, r the radius, and Q_a the absorption efficiency. Explicitly, the first solution method Eq. (4) becomes

$$\bar{g} = \int_0^\infty g(k + k_p) f(k) dk \quad (24)$$

and the second solution Eq. (14) becomes

$$\bar{g} = \int_0^\infty h(s) T(s) e^{-k_p s} ds \quad (25)$$

Example No. 1: One-Dimensional Two-Flux vs Hybrid Three-Dimensional Approximation

When selecting a technique for performing plume radiance calculations, one usually wishes to select an appropriate method based upon an engineering tradeoff between accuracy and simplicity. Therefore, we show how, using the Space Shuttle SRB as an example, one might use the rigorous solution to choose between two approximate radiative transport models, a two-flux vs a hybrid model. The two-flux approximation considered here is not the version considered by Vanderbilt and Slack,¹⁶ but instead performs a rigorous band model spectral average of the full transport equation. Its only limitation is geometrical; it is strictly one-dimensional; the emphasis in the hybrid method is reversed; and it is fully three-dimensional. Its only limitation is the lack of proper spectral averaging of the higher-order terms referred to in Eq. (10). We now show that the two-flux approximation is actually more accurate for the Space Shuttle SRB.

The specific version of the two-flux approximation we consider replaces the continuous scattering phase function $P(\Omega)$ by two delta functions in the forward (0 deg) and backward (180 deg) directions. It is a one-dimensional approximation to the full three-dimensional problem, which greatly simplifies the numerics of the radiative transport calculation. The solution for the monochromatic two-flux emissivity is a simple analytic expression.³² This expression was extended to a band model result by spectral averaging in the transform domain according to Eq. (12). The conditions were identical to those of the previous calculations. The two-flux method requires specification of a backscatter fraction b . Some ambiguity occurs because this parameter can be specified in several ways.³³ A value of 0.3 was used based upon the 0.7 asymmetry factor of the Henyey-Greenstein scattering phase function. Since the band model spectral average is performed correctly, all of the error in the two-flux example can be attributed to the one-dimensional approximation. As can be seen from Fig. 6, the

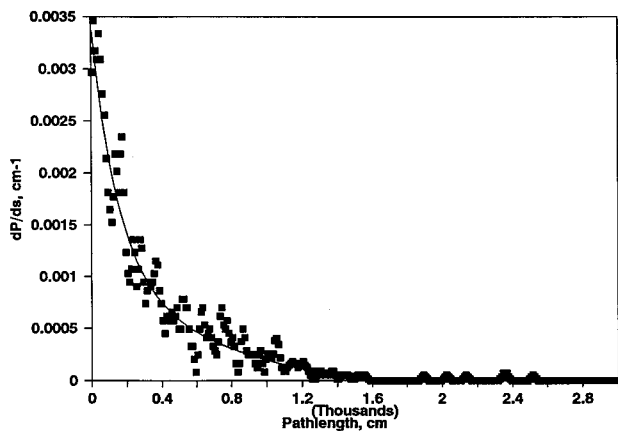


Fig. 5 Path length distribution $dP(s)/ds$.

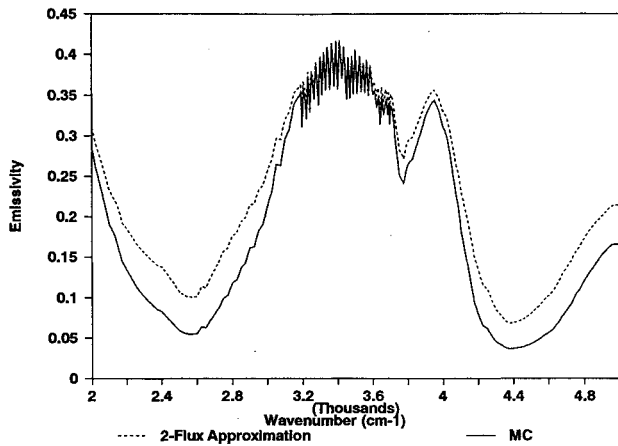


Fig. 6 Rigorous and two-flux approximation comparison.

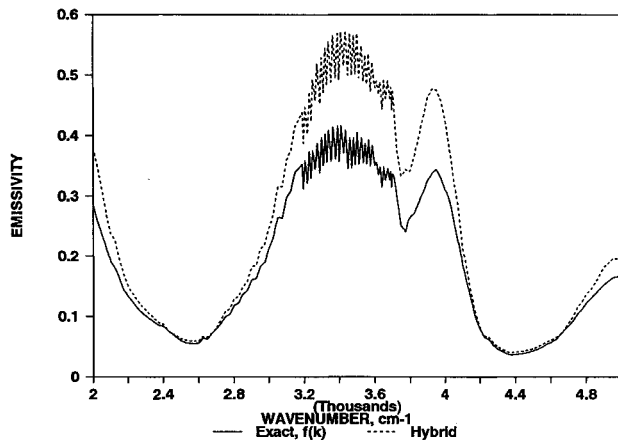


Fig. 7 Rigorous vs hybrid three-dimensional solution.

two-flux model does surprisingly well. The Monte Carlo result is the solution 1 from Fig. 4. The two-flux solution describes the intensity well near the center of the water band, but overpredicts the intensity in the wings. No attempt was made to minimize the error by appropriate choice of the backscatter coefficient b . However, this sort of optimization is clearly feasible.

We now consider the hybrid three-dimensional approximation. This approximation performs a correct band model spectral average only for the unscattered emissivity ε_u . It approximates the scattered (i.e., three-dimensional) emissivity ε_s using Beer's law and mean gas opacity within the band κ :

$$\varepsilon = \overline{\varepsilon_u(k)} + \varepsilon_s(\kappa) \quad (26)$$

Since the hybrid model uses exactly the same three-dimensional scattering phase function as the Monte Carlo calculation, all of the error can be attributed to the lack of proper band modeling in the scattered radiance term. As can be seen from Fig. 7, the hybrid approximation actually does worse than the two-flux method. Although the intensity in the band wings is well described, this is more than offset by the overprediction in the center of the band. As in Fig. 6, the Monte Carlo standard is the solution 1 of Fig. 4. The reason for the poor performance of the hybrid model is evident when one examines the curve of growth, Fig. 8. As can be seen, the hybrid model has an unphysical curve of growth. Specifically, the emissivity fails to increase monotonically with respect to opacity. Since at least one widely used code¹⁸ is based upon this approach, further investigation is warranted. The benchmark rigorous solution we provide is for a simplified homogeneous plume, so the actual performance of the two-flux and hybrid methods for the full inhomogeneous and non-isothermal plume remains unknown. For the case at hand,

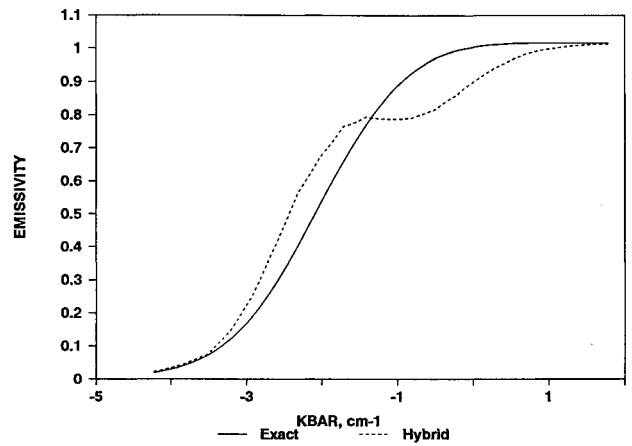


Fig. 8 SRB band model curve of growth.

the overall conclusion is that it is actually more important to correctly model the higher-order correlation terms in the transport equation [i.e., Eq. (10)] than to model the three-dimensional nature of the radiation transport. This is probably a consequence of the high optical depth and forward scattering nature of the Space Shuttle exhaust particles. Nevertheless, the case is an important one and common to large boosters.

Example No. 2: Approximation for Unequal Gas and Particle Temperatures

In this section the accuracy of a commonly used approximation is evaluated. Aluminum oxide droplets in rocket exhaust plumes are often several hundred K hotter than the gas. In this case the source function is no longer simply the Planck function. For the monochromatic case, and for a single particle group at a temperature T_p and gas at another temperature T_g , the source function becomes

$$(1 - \omega_p)[\gamma_p B(T_p) + (1 - \gamma_p)B(T_g)] + \omega_p \int P(\Omega - \Omega') I(\Omega') d\Omega' \quad (27)$$

where $B(T)$ is the Planck function. The factor g_n is the ratio of particle absorption to total particle plus gas absorption:

$$\gamma_p = n\sigma_p / (n\sigma_p + k_g) \quad (28)$$

Whereas, a rigorous band model formulation requires a proper spectral average of γ_p , the usual procedure for plume calculations is to approximate it using an uncorrelated mean value $\gamma(k)$

$$\gamma(k) = n\sigma_p / (n\sigma_p + \kappa) \quad (29)$$

where k is the average value of k_n over the spectral band. It is clear from the form of Eq. (28) that the error involved in the approximation Eq. (29) will tend toward zero in the limiting cases of $\gamma_p = 0$ (pure gas) or 1 (pure particles), and be maximum at some intermediate value. To our knowledge, however, the specific size and nature of this error has never been carefully assessed. Therefore, as a last example, we show that Eq. (29) is a useful approximation for the Space Shuttle SRB and that the maximum error is only a few percent.

The plume conditions and line of sight for this example were identical to the previous ones, except that a nonequilibrium particle temperature was specified. Specifically, the gas temperature was 2400 K, but the aluminum oxide droplet temperature was raised to 2800 K. This is an upper bound, because the particles are not believed to be this hot in the actual plume. Instead of plotting spectra, we chose a single fixed wavelength in the 3700-cm⁻¹ H₂O band, and varied the gas absorber amount from zero to a very large number. The

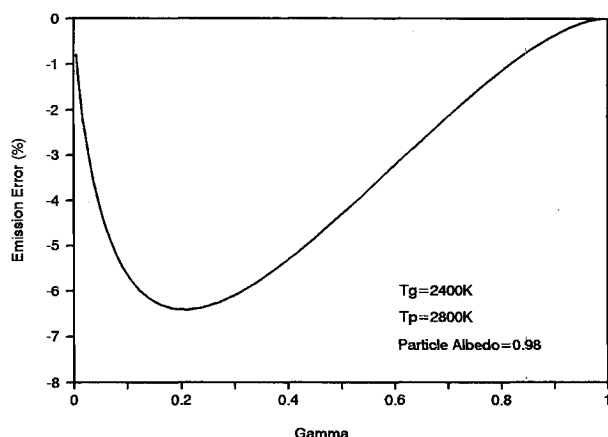


Fig. 9 Accuracy of approximation for unequal particle and gas temperatures.

particle absorption was held constant at a value corresponding to a single scattering albedo of 0.98. We therefore investigated the accuracy of the approximation Eq. (29) over the full range of radiation transport from the gas-dominated to the particle-dominated regime. Emissivities were computed using both the correct [Eqs. (27) and (28)] and the approximate [Eq. (29)] source function. As can be seen from Fig. 9, the maximum error of about 5% occurred near $\gamma \gg 0.2$. From Fig. 2, it can be inferred that comparable values of γ , will occur in the 3700 cm^{-1} water band of the SRB. In terms of the overall error budget, including uncertainties in thermophysical properties of the plume, this error is small. The approximation is therefore useful, and efforts to use the exact approach embodied in Eqs. (27) and (28) are not warranted.

Summary

The conventional infrared band model formalism for hot combustion gas radiation has not been rigorously extended to situations where scattering is important, such as in the exhaust plumes of aluminized solid propellant rockets. Practical calculations of plume radiative heating have therefore proceeded, based upon various approximations to the full radiative transport equation. The errors incurred by these approximations are difficult to ascertain because of the lack of rigorous validation cases. In addition, even when one has the freedom to choose certain parameters in the approximations, there are no clear optimization criteria. To help remedy these deficiencies, two different rigorous solutions have been developed. The first solution is based upon replacing the traditional band model average in the frequency domain by an equivalent average in the absorption coefficient domain, and involving the probability distribution of the absorption coefficient. This method was suggested by Domoto.¹⁵ The second solution is essentially the Laplace transform version of this result. Its principal advantage is that it expresses the final result in terms more closely related to conventional infrared band models. The equivalence of these two solutions was demonstrated with synthetic $2000\text{--}5000\text{ cm}^{-1}$ water vapor spectra of the Space Shuttle SRB exhaust plume. At present, both solutions are restricted to homogeneous media.

The usefulness of a rigorous solution to the transport equation was demonstrated with a lifelike example involving a choice between two alternative approximations for radiative heat transfer—a one-dimensional two-flux vs a hybrid three-dimensional model. Comparison against the rigorous solution demonstrated that the simpler two-flux model was actually superior for the Space Shuttle. As a second example, the rigorous solution was used to evaluate a commonly used approximation for the case of unequal particle and gas temperatures. This approximation was found to be accurate to within about 5% for the Space Shuttle SRB.

Acknowledgments

The authors wish to thank W. K. McGregor of Sverdrup Technology, AEDC Group, and D. Mann of the Army Research Office for suggesting this problem. W. Malkmus of Photon Research Associates, A. Mason and C. Peters of the University of Tennessee Space Institute, and Chad Limbaugh of Sverdrup Technology, AEDC Group provided helpful discussions.

References

- ¹Ludwig, C. B., Malkmus, W., Reardon, J. E., and Thomson, J. A. L., *Handbook of Infrared Radiation from Combustion Gases*, NASA SP3080, 1973.
- ²Young, S. J., "Band Model Formulation for Inhomogeneous Optical Paths," *Journal of Quantitative Spectroscopy & Radiative Transfer*, Vol. 15, 1975, pp. 483–501.
- ³Limbaugh, C. C., "The Infrared Emission-Absorption Method for Temperature and Species Partial Pressure Determination in Flames and Plumes," *Infrared Methods for Gaseous Measurements: Theory and Practice*, edited by J. Wormhoudt, Marcel Dekker, New York, 1985, pp. 197–243.
- ⁴Bernstein, L. S., Robertson, D. C., and Conant, J. A., "Band Model Parameters for the $4.3\text{ }\mu\text{m}$ CO_2 Band from 200 to 3000 K," *Journal of Quantitative Spectroscopy & Radiative Transfer*, Vol. 23, 1980, pp. 169–185.
- ⁵Hermesen, R. W., "Aluminum Oxide Particle Size for Solid Rocket Motor Performance Prediction," *Journal of Spacecraft and Rockets*, Vol. 18, No. 6, 1981, pp. 483–490.
- ⁶Bohren, C. F., and Huffman, D. R., *Absorption and Scattering of Light by Small Particles*, Wiley Interscience, New York, 1983.
- ⁷Krishnan, S., Weber, J. K. R., Schiffman, R. A., Nordine, P. C., and Reed, R. A., "Refractive Index of Liquid Aluminum Oxide at $0.6328\text{ }\mu\text{m}$," *Journal of the American Ceramic Society*, Vol. 74, No. 4, 1991, pp. 881–883.
- ⁸Gryvnak, D. A., and Burch, D. E., "Optical and Infrared Properties of Al_2O_3 at Elevated Temperatures," *Journal of the Optical Society of America*, Vol. 55, No. 6, 1965, pp. 625–629.
- ⁹Abrevaya, H., and Nordine, P. C., "Evaporation and Energy Transfer for a Partially Molten, Laser-Heated Sapphire Filament," *Journal of the American Ceramic Society*, Vol. 7, No. 7, 1988, pp. 546–553.
- ¹⁰Konopka, W. L., Reed, R. A., and Calia, V. S., "Infrared Optical Properties of Al_2O_3 Rocket Particles," *Spacecraft Contamination: Sources and Prevention*, edited by J. A. Roux and T. D. McCay, Vol. 91, Progress in Astronautics and Aeronautics, AIAA, New York, 1984, pp. 180–196.
- ¹¹Oliver, S. M., and Moylan, B., "An Analytical Approach for the Prediction of Gamma-to-Alpha Phase Transformation of Aluminum Oxide Particles in the Space Shuttle ASRM and RSRM," AIAA Paper 92-2915, July 1992.
- ¹²Toon, O. B., Pollack, J. B., and Khare, B. N., "The Optical Constants of Several Atmospheric Aerosol Species: Ammonium Sulphate, Aluminum Oxide, and Sodium Chloride," *Journal of Geophysical Research*, Vol. 81, No. 33, 1976, pp. 5733–5748.
- ¹³Thomas, M. E., Joseph, R. I., and Tropf, W. J., "Infrared Transmission Properties of Sapphire, Spinel, Yttria, and AlON as a Function of Temperature and Frequency," *Journal of the Optical Society of America*, Vol. 27, No. 2, 1988, pp. 239–245.
- ¹⁴Malkmus, W., "Some Comments on the Extension of Band Models to Include Scattering," *Journal of Quantitative Spectroscopy and Radiative Transfer*, Vol. 40, 1988, pp. 201–204.
- ¹⁵Domoto, G. A., "Frequency Integration for Radiative Transfer Problems Involving Homogeneous Non-Gray Gases: The Inverse Transmission Function," *Journal of Quantitative Spectroscopy & Radiative Transfer*, Vol. 14, 1974, pp. 935–942.
- ¹⁶Vanderbilt, D., and Slack, M. W., "A Model for Emission and Scattering of Infrared Radiation from Inhomogeneous Combustion Gases and Particles," Grumman Aerospace Corp., Grumman RM-621, Bethpage, New York, June 1976.
- ¹⁷Schuster, A., "Radiation Through a Foggy Atmosphere," *Astrophysical Journal*, Vol. 21, 1905, p. 1; see also *Selected Papers on the Transfer of Radiation*, edited by D. H. Menzel, Dover, New York, 1966.
- ¹⁸Ludwig, C. B., Malkmus, W., Freeman, G. N., Slack, M. W., and Reed, R. A., "A Theoretical Model for Absorbing, Emitting, and Scattering Plume Radiation," *Spacecraft Radiative Transfer and Temperature Control*, edited by T. E. Horton, Vol. 83, Progress in Astronautics and Aeronautics, AIAA, New York, 1982; see also

AIAA Paper 81-1051, June 1981.

¹⁹Chu, C. M., and Churchill, S. W., "Numerical Solution of Problems of Multiple Scattering of Electromagnetic Radiation," *Journal of Physical Chemistry*, Vol. 59, 1955, pp. 855-863.

²⁰Meador, W. E., and Weaver, W. R., "Six-Beam Models in Radiative Transfer Theory," *Applied Optics*, Vol. 15, No. 12, 1976, pp. 3155-3160.

²¹Everson, J., and Nelson, H. F., "Development and Application of a Reverse Monte Carlo Radiative Transfer Code for Rocket Plumes," AIAA Paper 93-0137, Jan. 1993.

²²Crosbie, A. L., and Linsenbardt, T. L., "Two-Dimensional Isotropic Scattering in a Semi-Infinite Medium," *Journal of Quantitative Spectroscopy & Radiative Transfer*, Vol. 19, March 1978, pp. 257-284.

²³Van De Hulst, H. C., *Multiple Light Scattering: Tables, Formulas, and Applications*, Academic Press, New York, 1980.

²⁴Beale, K. S., Reed, R. A., Daugherty, T. L., Oliver, S. M., Simmons, M. A., and McGregor, W. K., "The Effect of Searchlight Emission on Radiation from Solid Rocket Plumes," AIAA Paper 92-2918, July 1992.

²⁵Henye, L. G., and Greenstein, J. L., *Astrophysical Journal*, Vol. 85, 1941, p. 70.

²⁶Kamiuto, K., "Study of the Henye-Greenstein Approximation to Scattering Phase Functions," *Journal of Quantitative Spectroscopy & Radiative Transfer*, Vol. 37, No. 4, 1987, pp. 411-413.

²⁷Maynard, C. W., "An Application of the Reciprocity Theorem to the Acceleration of Monte Carlo Calculations," *Nuclear Science and Engineering*, Vol. 10, 1961, pp. 97-101.

²⁸Walters, D. V., and Buckius, R. O., "Rigorous Development for Radiation Heat Transfer in Nonhomogeneous Absorbing, Emitting, and Scattering Media," *International Journal of Heat and Mass Transfer*, Vol. 35, No. 12, 1992, pp. 3323-3333.

²⁹Marchuk, G. I., Mikhailov, G. A., Nazaraliev, M. A., Darbinjan, R. A., Kargin, B. A., and Elepov, B. S., *The Monte Carlo Methods in Atmospheric Optics*, Springer-Verlag, New York, 1980.

³⁰Pearce, B. E., Wurster, W. H., Flanigan, M. C., Smolarek, K. K., and Huang, R., "Predictions and Measurements of Radiation Base Heating from a Solid Propellant Rocket Motor Plume," AIAA Paper 91-1431, June 1991.

³¹Malkmus, W., "Random Lorentz Band Model with Exponential-Tailed s^{-1} Line Intensity Distribution," *Journal of the Optical Society of America*, Vol. 57, No. 3, 1967, pp. 323-329.

³²Bartky, C. D., and Bauer, E., "Predicting the Emittance of a Homogeneous Plume Containing Alumina Particles," *Journal of Spacecraft and Rockets*, Vol. 3, No. 10, 1966, pp. 1523-1527.

³³Koenigsdorff, R., Miller, F., and Ziegler, R., "Calculation of Scattering Fraction for Use in Radiative Flux Models," *International Journal of Heat and Mass Transfer*, Vol. 34, No. 10, 1991, pp. 2673-2676.